Geophys. J. Int. (2002) **150,** 422–439

Offset on the Main Recent Fault of NW Iran and implications for the late Cenozoic tectonics of the Arabia–Eurasia collision zone

Morteza Talebian and James Jackson

University of Cambridge, Department of Earth Sciences, Bullard Laboratories, Madingley Road, Cambridge CB3 OEZ, *UK*
E-mails: talebian@esc.cam.ac.uk; jackson@esc.cam.ac.uk

Accepted 2002 February 6. Received 2002 January 8; in original form 2001 June 29

SUMMARY

We use drainage patterns, geological markers and geomorphological features to determine a right-lateral offset of ∼50 km, and possibly as much as ∼70 km, on the Main Recent Fault in NW Iran. This fault trends NW–SE and forms the NE border of the Zagros mountains. It accommodates the strike-slip component of the N–S convergence between Arabia and Eurasia, with the NE–SW shortening component being accommodated in the Zagros Fold Belt. Its ∼50 km strike-slip offset implies a shortening of ∼50 km in the fold belt and ∼70 km total N–S convergence accommodated in the NW Zagros. This is a substantial fraction of the 85–140 km overall Arabia–Eurasia convergence expected over the last 3–5 Ma. If the Main Recent Fault initiated at that time, as seems likely from geological arguments, it has a horizontal slip rate of at least 10–17 mm $yr^{-1}$and should be the source of frequent earthquakes of M_s 6–7, as has been seen in the 20th century and the earlier historical record. The similarity of the offsets and probable ages of the North Anatolian and Main Recent Faults suggests that they have been active as an almost continuous zone of right-lateral shear on the north edge of the Arabian and Anatolian plates since the early Pliocene.

Key words: active faulting, earthquakes, Iran, Middle East, seismotectonics.

1 INTRODUCTION

The purpose of this paper is to estimate the right-lateral offset on the Main Recent Fault, a major strike-slip fault system in NW Iran and one of the key structural elements in the active tectonics of the Middle East. The Main Recent Fault strikes NW–SE and can be traced as a narrow, linear series of fault segments from near the Turkey–Iran border at 37°N for over 800 km to the SE (Fig. 1). Right-lateral strike-slip faulting also continues NW in a broader zone through eastern Turkey to eventually join the North Anatolian Fault, thus forming a band of right-lateral shear linking Iran and Turkey. While a lot is now known concerning the slip rate and offsets on the North Anatolian Fault in Turkey (Şengör *et al.* 1985; Barka 1992; Armijo *et al.* 1999; McClusky *et al.* 2000), much less is known about the Main Recent Fault in Iran.

We will first use drainage patterns to estimate offsets on the Main Recent Fault, and compare these offsets with displaced geological markers. We do this in a region of NW Iran near Kermanshah (Fig. 2), where a series of earthquakes in the last century help guide us to the precise location and nature of the faulting. It is much more difficult to estimate the ages of the offsets and hence the slip rate on the fault, though various inferences can be made from the geological history. We will show that the offset on the Main Recent Fault is similar to that on the North Anatolian Fault and if, as we suspect, the two faults initiated at roughly the same time, this allows us to estimate a plausible slip rate on the Main Recent Fault and to assess its significance in the Eurasia–Arabia collision. There are two motivations for this work. One is the need to have some idea of the slip rates on major faults to assess the seismic hazard they represent. The other is more subtle. Eventually we will have reliable short-term estimates of slip rates on most major faults through GPS measurements, although these are not yet available in Iran. At that point we will want to see how far back in time we can extrapolate those slip rates before we account for, or run into conflict with, the observed geological structure or fault offsets. That question moves beyond asking what is the present-day configuration and rate of deformation (the goal of much seismotectonic research for the last 30 years), to asking whether today's patterns and rates of faulting can also account for the finite, cumulative deformation. Not only is this question essential for understanding how the Arabia–Eurasia convergence has been accommodated in the mountains that now separate them, but it is also a central issue in continental mechanics (e.g. McKenzie & Jackson 1983; Molnar & Gipson 1994; Jackson 1999). To address it, we need to know the total offsets on the major faults.

2 TECTONIC AND GEOLOGICAL BACKGROUND

2.1 Regional tectonics

Whereas the North Anatolian and Main Recent Faults are relatively continuous linear features, the strike-slip faulting in eastern Turkey

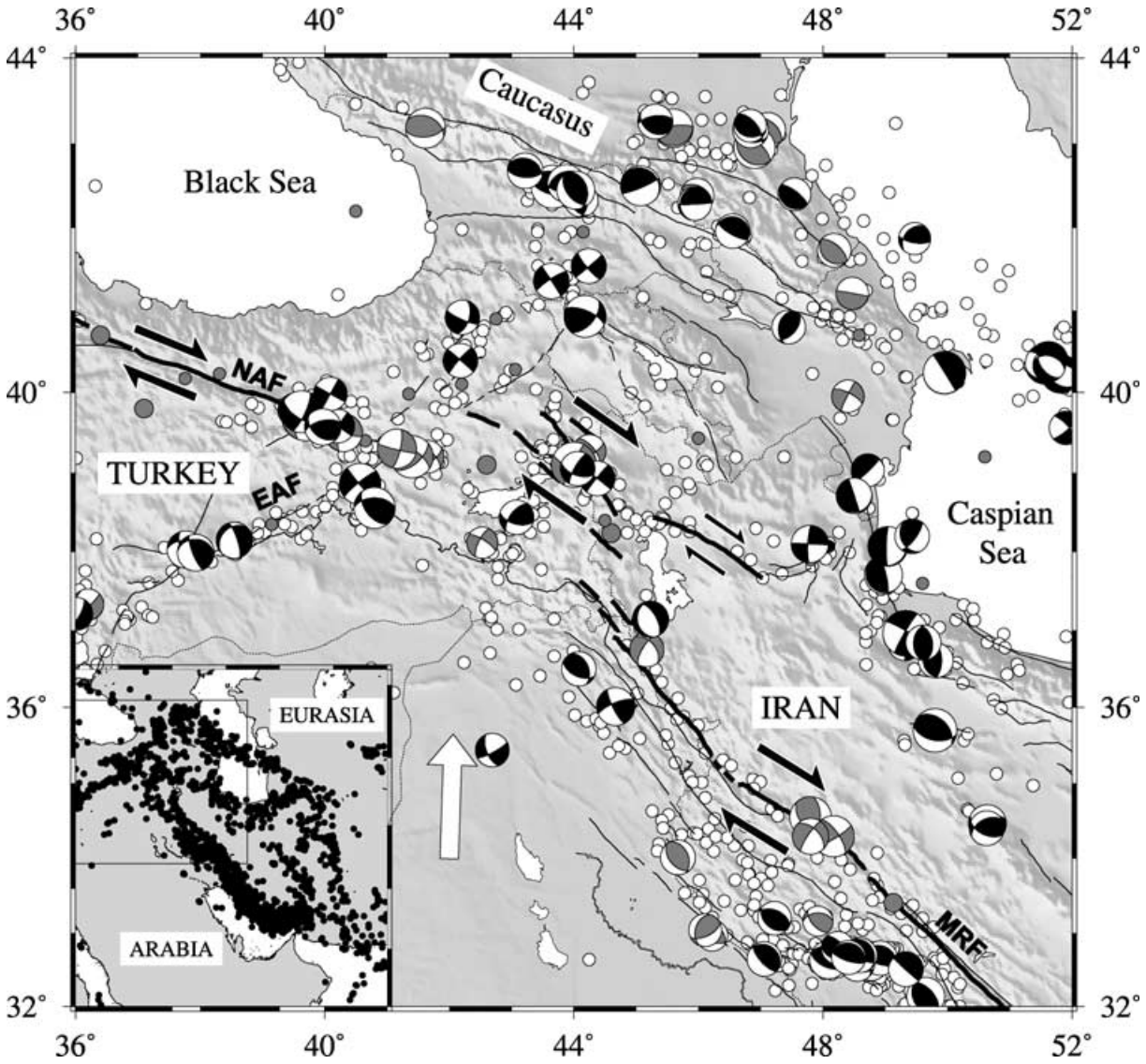

Figure 1. Summary seismotectonic map of NW Iran, eastern Turkey and the Caucasus. Major active faults are shown as black lines, with thicker lines emphasizing the system of NW–SE right-lateral strike-slip faults that joins the North Anatolian Fault (NAF) in the NW with the Main Recent Fault (MRF) in the SE. EAF is the East Anatolian Fault. Fault plane solutions in black are from the Harvard CMT catalogue (http://www.seismology.harvard.edu/CMTsearch.html) or determined by long-period body-wave modelling (catalogue in Jackson 2001). Lighter-coloured focal mechanisms are first motion fault plane solutions, from Jackson & McKenzie (1984). White dots in the main figure and black dots in the inset are earthquake epicentres during the period 1964 to 1998 from Engdahal *et al.* (1998). The white arrow shows the direction of Arabia–Eurasia convergence at 34°N 42°E. Grey dots (small and large) are epicentres of other earthquakes larger than M_s 6.0 and 7.0 between 1900 and 1963.

is discontinuous and fragmented, with shorter fault segments distributed over a zone perhaps 200 km wide (Fig. 1). This contrast probably arises because the Arabia–Eurasia convergence, which is roughly N–S at ∼25–30 mm yr^{-1}at this longitude, is oblique to the NW–SE trend of the orogenic belt (Jackson 1992; De Mets *et al.* 1994; Chu & Gordon 1998). The strike-parallel and strike-normal components of this oblique shortening appear to be spatially separated on to different subparallel faults with orthogonal slip vectors, which can be seen in both the earthquake focal mechanisms (Jackson 1992; Jackson & Ambraseys 1997) and the GPS velocity field (McClusky *et al.* 2000). However, the shortening component is taken up south of the North Anatolian Fault (in SE Turkey) and predominantly south of the Main Recent Fault (in the Zagros), whereas it occurs north of the strike-slip faulting between the two (in the Caucasus). This arrangement is unstable, in that the strike-slip faulting in eastern Turkey and NW Iran must be moving north relative to Eurasia because of the shortening in the Caucasus, whereas the North Anatolian and Main Recent Faults need not do so (Jackson 1992). The configuration of the separated or 'partitioned' components of oblique shortening therefore precludes a continuous right-lateral strike-slip fault along the line of the North Anatolian and Main Recent Faults. Thus the North Anatolian and Main Recent Faults perform rather similar functions in the present-day tectonics of the Arabia–Eurasia collision zone.

2.2 Geology

The Main Recent Fault was first identified from offset drainage features by Wellman (1966), and was then later described in more detail and named by Tchalenko & Braud (1974). It borders the NE edge

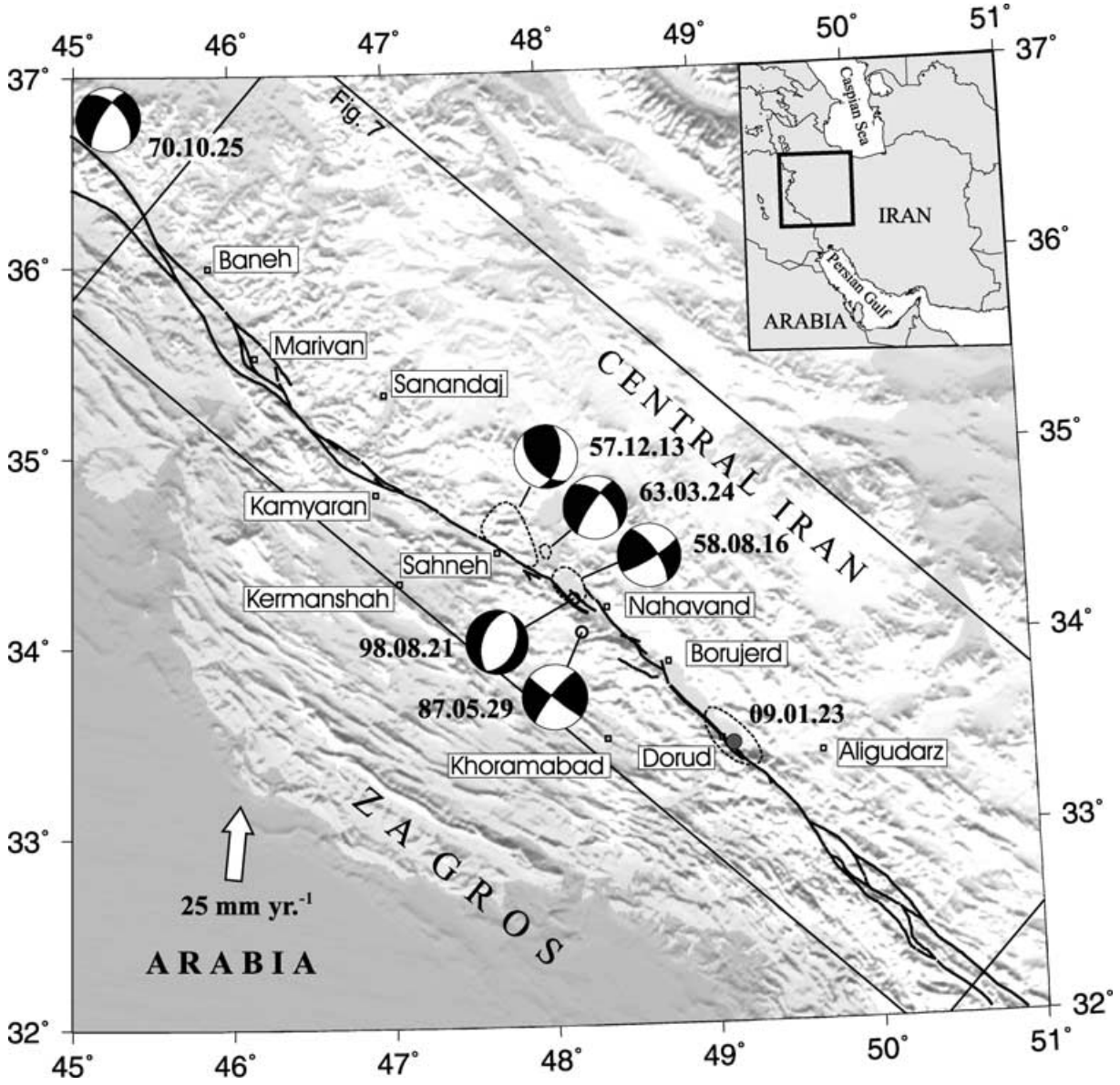

Figure 2. Map of the part of the Main Recent Fault system that is the focus of this study, between 36°N and 32°N. Focal mechanisms are listed in Table 1, with the macroseismic regions of the earthquakes of 1909, 1957, 1958 and 1963 outlined by dotted lines. Fault traces are based on Tchalenko & Braud (1974) and on our own inspection of satellite imagery. The white arrow shows the overall Arabia–Eurasia convergence at 33°N 46°E. The box outlines the region of Fig. 7.

of the Zagros mountains, approximately following an important geological boundary called the 'Zagros suture', the 'Zagros Thrust Line' or the 'Main Zagros Reverse Fault' by various authors (e.g. Stöcklin 1974; Falcon 1974; Berberian 1995), which approximately separates the rocks of the Arabian continental margin to the SW from metamorphic and volcanic rocks of central Iran to the NE (e.g. Berberian & King 1981). This geological boundary is also an important seismotectonic feature today, marking an abrupt cut-off between the intense seismicity of the Zagros and the almost aseismic central Iran plateau (Fig. 1, inset). The Main Recent Fault roughly follows the NE border of the NW–SE trending High Zagros Thrust Belt (Falcon 1974; Berberian 1995), which has the highest topography and rainfall in the region. Peaks reach heights of 4000 m and gorges reveal deeper exposures into the cores of thrusted anticlines (reaching lower Paleozoic levels) than elsewhere in the Zagros. This part of the Zagros has been uplifted by steep NE-dipping reverse faults to the SW, and is deeply dissected by the drainage. Some shortening occurred in the High Zagros in the Late Cretaceous, at which time ophiolitic rocks and deep sea sediments were emplaced on to the Arabian margin, particularly in the Kermanshah region, which is the focus of this report (Stoneley 1976). These exotic rocks are potentially useful markers for measuring offsets on the Main Recent Fault, which otherwise is subparallel to most of the geological structure.

However, ophiolite emplacement preceded the final suturing of Arabia with central Iran, which probably began in the Miocene (Stoneley 1981). Moreover, the main shortening of the Arabian margin in the Zagros, including all of the Simple Folded Belt SW of the High Zagros, began even later in the Pliocene, probably only 3–5 Ma (Falcon 1974). This is also close to the time at which there

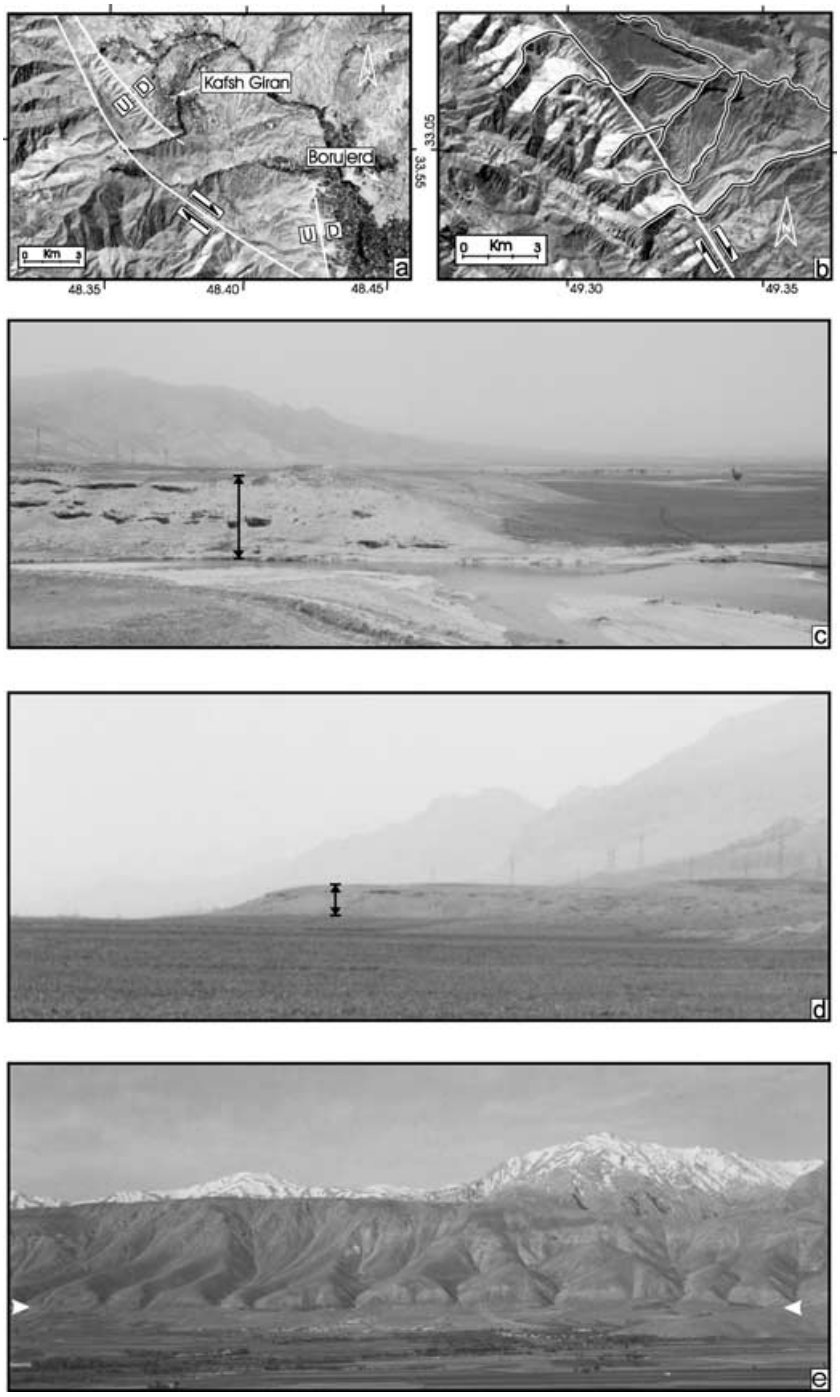

Figure 3. (a) Detail of a LANDSAT image near Borujerd, showing two subparallel NW–SE fault traces, both of which have vertical components down to the NE, causing their SW sides to be incised by drainage. The roughly N–S fault to the south of Borujerd marks the NW end of the Borujerd–Dorud basin. (b) Detail of a LANDSAT image showing the Main Recent Fault trace SE of Dorud, where a right-lateral offset of ∼1 km is clear in the drainage. (c) The main fault scarp bounding the west side of the Dorud basin, where the Sardeh River crosses the fault at 33°44.3′N 48°46.7′E. The view is to the north. Note the uplifted river terraces on the west side of fault, at a height (black arrow) of 10–15 m above the river. The surface ruptures in the 1909 earthquake in part followed this escarpment. (d) View south of the Dorud escarpment taken from a few km north of Fig. 3(c). Again, the fault appears as a linear scarp uplifting the flat terraces of the Sardeh River (black arrows). (e) View looking SW towards the NE of the two parallel fault scarps in Fig. 3(a). The cultivated region in the foreground is the village of Kafsh Giran at 33°56′N 48°37′E. Note the classic triangular facets ('flat-irons') with deeply incised wine-glass shaped canyons along the range front, caused by vertical motion and suggesting an extensional (normal) slip component.

is a major reorganization of the sedimentation and deformation in the South Caspian Basin (Devlin *et al.* 1999; Jackson *et al.* 2002). We suspect that this time represents the final closure of the minor oceanic and marginal basins that make up central Iran (Berberian & King 1981; McCall 1996) and the onset of true intracontinental shortening. We also expect that the present-day configuration of the active faulting in Iran dates from roughly that time. A similar geological history is seen further west. Although there is some

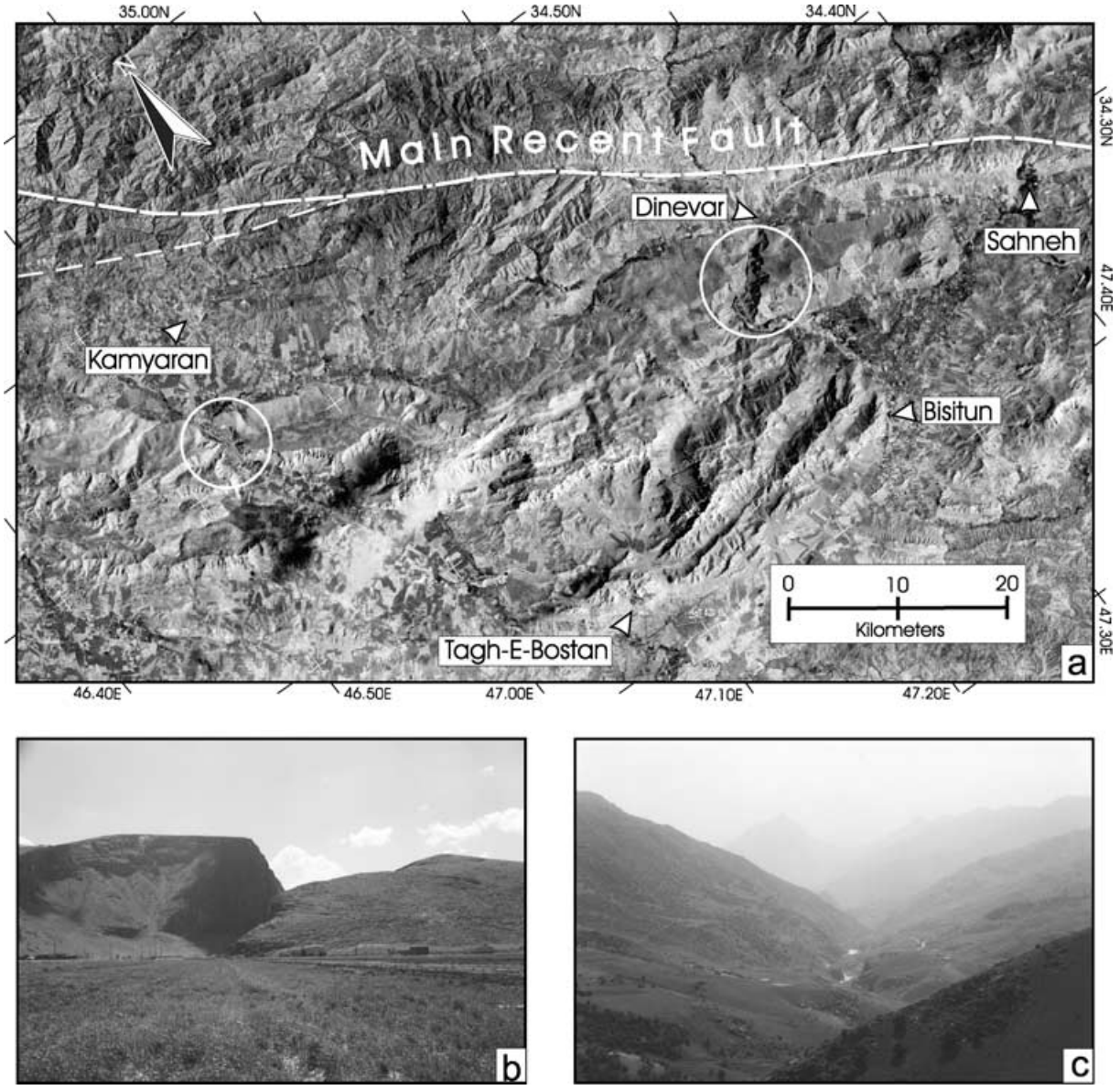

Figure 4. Examples of gorges in the river systems crossing the Main Recent Fault. (a) LANDSAT image of the two gorges at Kamyaran and Dinevar (ringed with white circles) that provide the exit points for streams draining to the SW. Our reconstruction in Fig. 7(b) is based on moving the streams that now drain through the Dinevar gorge back to a position through the Kamyaran gorge. The incised valley at Sahneh, now isolated from its original catchment, is also indicated (see Fig. 11). The traces of the Main Recent Fault system are marked by white lines. (b) The entrance to the gorge at Dinevar, looking south, at 34°34′N 47°26′E. (c) View south along the gorge at Dorud, at 33°28′N 49°04′E.

evidence for early Tertiary collision in eastern Turkey (Hempton 1987), much of the broader collision zone did not start to deform until the mid-Miocene or later (Dewey *et al.* 1986). It is also probable that most of the offset on the North Anatolian Fault was achieved over the last 5 Ma (see the later discussion).

2.3 Earthquakes

Several significant earthquakes occurred on or near the Main Recent Fault over the last 100 yr (Fig. 2, Table 1). The largest of these was in 1909 ($M_s = 7.4$) and produced at least 45 km of surface ruptures, downthrown to the NE and following the SW side of the Borujerd–Dorud depression (Ambraseys & Moinfar 1973; Tchalenko & Braud 1974). The vertical component of the 1909 scarps is reflected in the geomorphology, with gorges, river terraces and abandoned stream channels all demonstrating longer-term relative uplift on the SW side of the fault (Figs 3c and d). It is unclear whether the 1957 ($M_s = 6.7$) earthquake produced surface ruptures other than local fissuring (Ambraseys *et al.* 1973; Tchalenko & Braud 1974). McKenzie (1972) shows a poorly constrained first-motion fault plane solution for the 1957 earthquake (Fig. 2), which suggests a substantial thrust component. Shirakova (1967) reports a similar mechanism, but shows no polarity data. The 1958 ($M_s = 6.6$) earthquake produced up to 20 km of discontinuous surface rupture along the SW side of the Nahavand–Firuzabad depression (see the detailed map in Fig. 9), again with the NE side downthrown (Ambraseys & Moinfar 1974a;

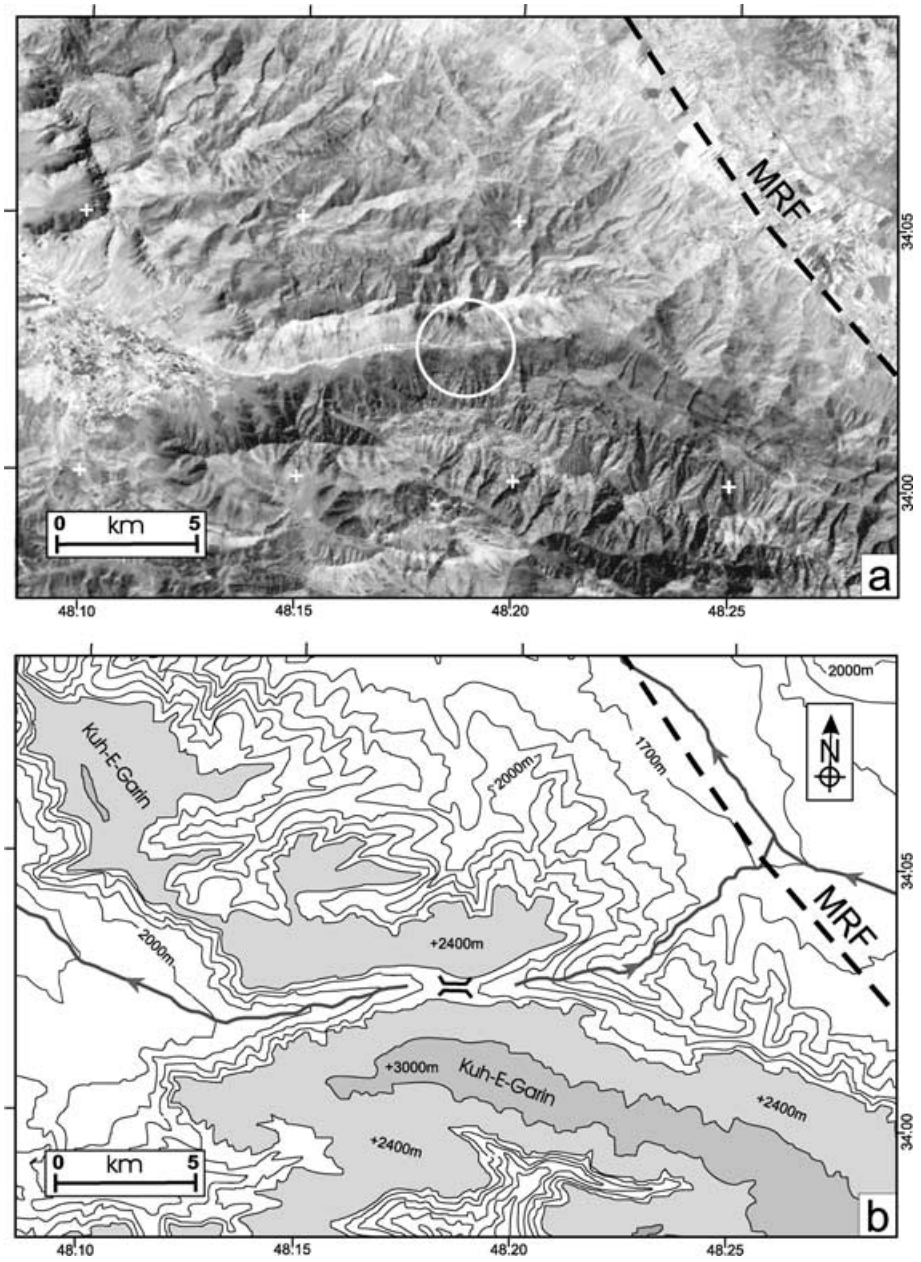

Figure 5. (a) LANDSAT image and (b) map of the dry valley south of Nahavand (marked G in Fig. 9a, and called Kuh-e-Sang Surakh). The pass itself is circled in (a) and marks the course of a river that once drained through the mountains from the NE side of the Main Recent Fault before uplift on the SW side of the fault caused the river course to be abandoned. See also Fig. 6.

Tchalenko & Braud 1974) and again reflecting the geomorphology, which shows clear evidence of longer-term uplift on the SW side. Shirakova (1967) reports a fault plane solution for the 1958 earthquake indicating NW–SE right-lateral strike-slip, but again without showing polarity data (Fig. 2). A smaller earthquake of $M_s = 5.8$ in 1963 also has a poorly constrained first-motion solution that is consistent with right-lateral strike-slip, perhaps with a normal component (Fig. 2; Jackson & McKenzie 1984). It produced no reported surface faulting (Ambraseys & Moinfar 1974b; Tchalenko & Braud 1974). The best-constrained focal mechanisms are for three smaller earthquakes, all of $M \sim 5$, in 1970, 1987 and 1998 (Fig. 2, Table 1), none of which can be definitely associated with a particular surface fault.

These earthquakes and their surface ruptures are important for two reasons. First, they confirm the right-lateral character of the fault system. Secondly, they indicate an important vertical component in places. Three of the focal mechanisms in Fig. 2 have normal components and two of the surface ruptures (in 1909 and 1958) follow basin-margin scarps that have a classical normal-fault morphology (Figs 3a, b and e). These indicate that at least some of the linear depressions, such as at Nahavand and Dorud, are structurally controlled, which is a feature we will exploit later. Those depressions are clearest where the fault system strikes $\sim 315^\circ$ between Nahavand and Dorud, and are absent where the fault strikes $\sim 300^\circ$ between Kamyaran and Sahneh. This is probably an indication that the regional slip vector, at least in the Kamyaran–Dorud

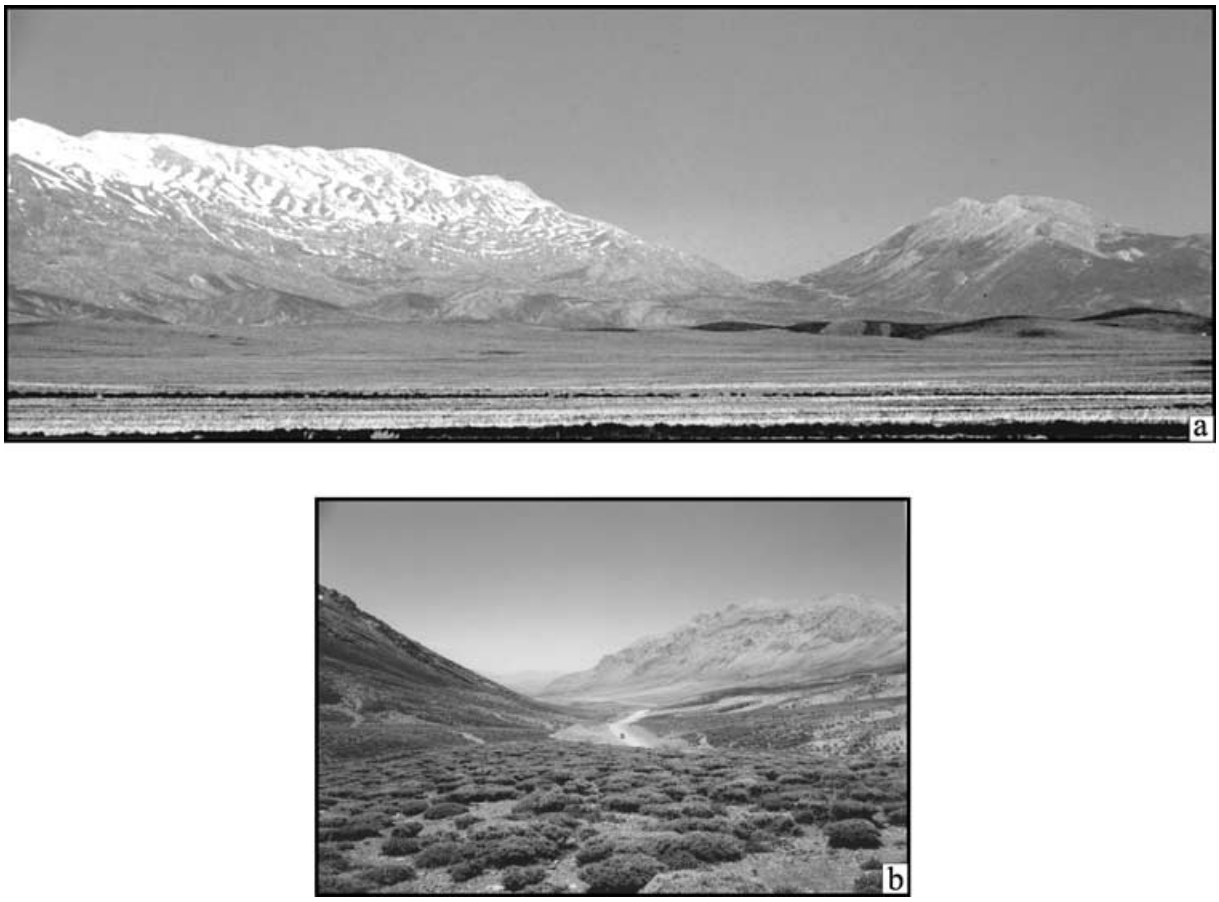

Figure 6. Two views of the dry valley at Kuh-e-Sang Surakh south of Nahavand in Fig. 5. (a) View looking west from the south end of the Nahavand basin. The dry valley is the low pass in the skyline. (b) View west at the watershed in the pass itself at 34°2.1′N 48°28.6′E.

area, is about 300°–310°. Other earthquakes are also known from this region prior to 1900 (Ambraseys & Melville 1982; Berberian & Yeats 2001).

3 METHODOLOGY AND APPROACH

The drainage provides the key that reveals the cumulative offset on the Main Recent Fault, as it does on other major strike-slip faults in Iran (e.g. Walker & Jackson 2002) and elsewhere (e.g. Replumaz *et al.* 2001). The High Zagros is crossed by rivers flowing SW to the Persian Gulf that originate from a drainage divide typically 50 km to the NE of the Main Recent Fault. Beyond that divide, rivers drain into the internal desert basins of central Iran or to the Caspian Sea. The rivers crossing the High Zagros occupy deep gorges on the SW side of Main Recent Fault (Fig. 4). These gorges form a small number of restricted exits to the drainage coming from the NE. As the offset on the Main Recent Fault increases, so the drainage on the NE side must either keep contact with its gorge or abandon it for another outlet. The gorge itself may receive different catchments from the NE over time, or it may become abandoned altogether, to

Table 1. Earthquakes near the Main Recent Fault 32–37°N.

Date	Time	Lat.	Long.	M_s	M_w	Strike	Dip	Rake	*sv*	Ref.
1909.01.23	0248	33.41	49.13	7.4						A
1957.12.13	0145	34.58	47.82	6.7		136	50	50		M
1958.08.16	1913	34.30	48.17	6.6		325	70	170	325	S
1963.03.24	1244	34.50	48.02	5.8		314	52	−165	304	J
1970.10.25	1122	36.77	45.13	4.8		319	50	−155	302	J
1987.05.29	0627	34.05	48.21		4.9	128	88	170	308	H
1998.08.21	0513	34.23	48.16		4.9	025	39	−84		H

Locations of earthquakes before 1970 are based on their macroseismic areas (Ambraseys & Melville 1982), as instrumental epicentres are seriously in error (Ambraseys 1978; Berberian 1979). The slip vector on the right-lateral plane of the strike-slip solutions is *sv*. The letter in the last column is the reference for each earthquake: A is Ambraseys & Melville (1982); M is McKenzie (1972); S is Shirakova (1967); J is Jackson & McKenzie (1984); and H is the Harvard CMT solution.

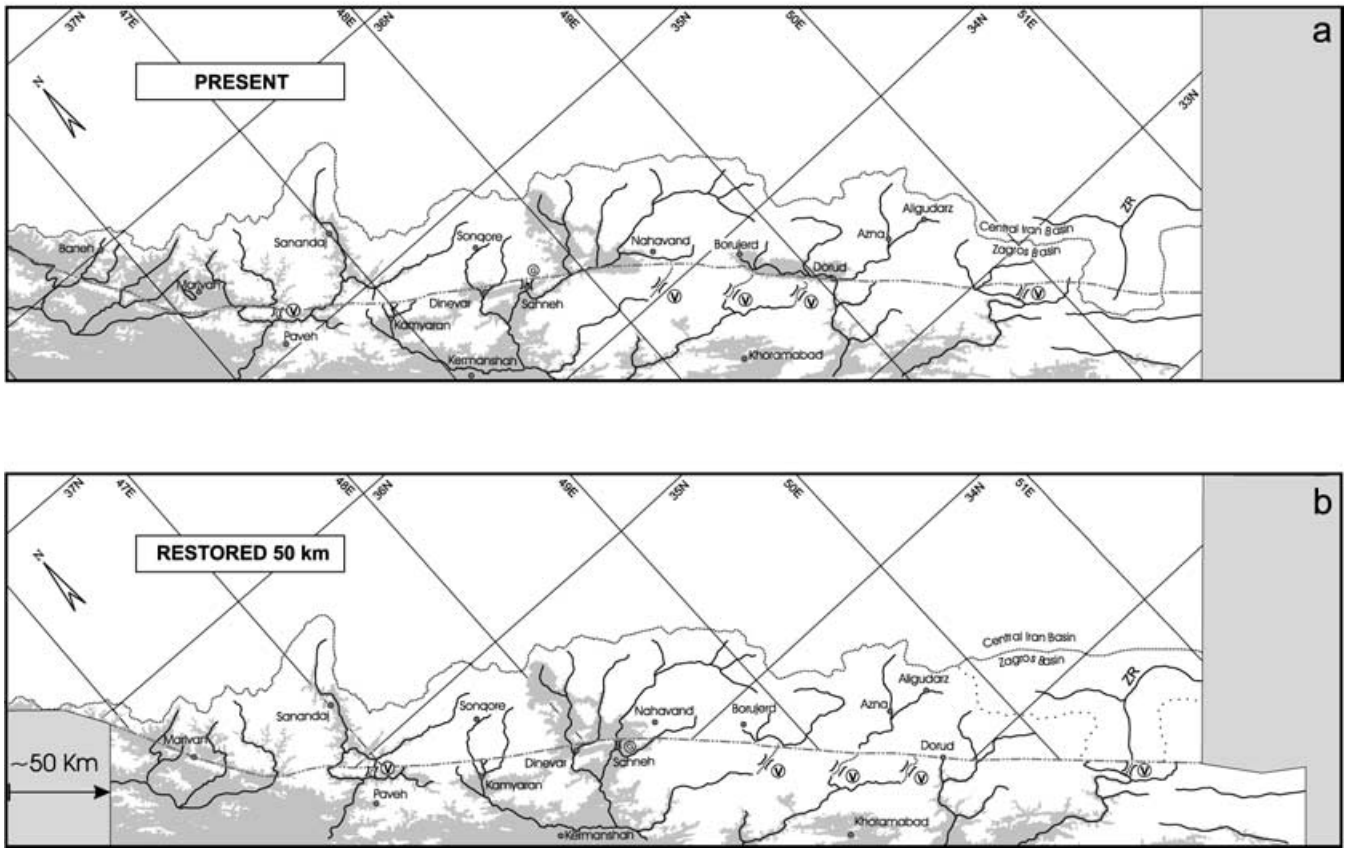

Figure 7. Present-day (a) and restored (b) drainage maps of the Main Recent Fault. The restoration involves an offset of ∼50 km (see the text for details). Dry valleys that are now abandoned, but which were once major water courses, are dotted and marked with V symbols. The incised valley at Sahneh (see Fig. 4a) is marked G. The dotted line in the NE is the main drainage divide separating rivers that flow to the Persian Gulf (Zagros basin) from those that flow NE to central Iran or the Caspian Sea. The approximate line of the Main Recent Fault, used for the reconstruction, is marked by a dashed line. ZR is the Zayandeh Rud river. The grey shaded area is below 1600 m elevation.

leave a dry valley (or 'wind gap') crossing the mountains, especially where the SW side of the fault is being uplifted today, such as near the 1958 and 1909 earthquakes (Figs 5 and 6). These features allow us to attempt a reconstruction of the offset on the fault, matching the drainage catchments in the NE to the different outlets on the SW. As we will see, the restored drainage pattern is much simpler than today, indicating a system of linear streams flowing SW from the Zagros–central Iran divide and removing some present-day anomalies. We will then compare our inferred offset on the fault with the geological evidence.

In making our reconstructions, we have to ensure that both sides of the Main Recent Fault remain in contact. The strike of the fault varies along its length, being about 330° near Marivan in the NW, 300° in the central part near Sahneh, and 315° in the SE near Dorud (Fig. 2). The central part of the fault zone is notable for being relatively narrow, linear and free from elongated fault-parallel basins on its NE side and from abandoned dry valleys on its SW side (Fig. 7a). In contrast, both the NW and SE sections contain low topography on the NE side (the Baneh–Marivan region, the Nahavand and Borujerd–Dorud basins) and abandoned dry valleys on the SW side (Fig. 7a). As mentioned above, we suspect that this reflects a regional slip vector that has a small extensional component in the NW and SE, with an azimuth close to that of the central section (∼300°–310°). In addition, the Dorud basin is associated with a small right-step in the faulting and is in a pull-apart location. Our interest here is in the strike-slip component of the offset, so we restored the three sections separately, allowing an overlap on the fault in the reconstruction of the northern Marivan section to compensate for what we expect is an extensional component in that region (Fig. 8a). In order for the three blocks south of the fault not to overlap (Fig. 8a), the restoration requires slightly different strike-slip offsets in each section because of their different azimuths, but this is a minor effect of no great significance.

4 RECONSTRUCTIONS OF THE MAIN RECENT FAULT

4.1 Evidence from drainage

Fig. 7(b) shows a reconstruction formed by restoring an offset of ∼50 km on the Main Recent Fault (52 km on the NW, 50 km on the central and 55 km on the SE sections). Although smaller-scale offsets of ∼1 km are visible at various places along the fault (e.g. Fig. 3b), the reconstructed offset of ∼50 km is the first major possible offset to investigate, because it is achieved by moving the Sonqore river, which currently exits through the Dinevar gorge, to the next gorge at Kamyaran (Figs 4, 7a and b). Between those two gorges is a high mountain wall with no drainage exits at all. We test whether this reconstruction is plausible by checking its effect on the drainage pattern at other points, which we now examine in some detail.

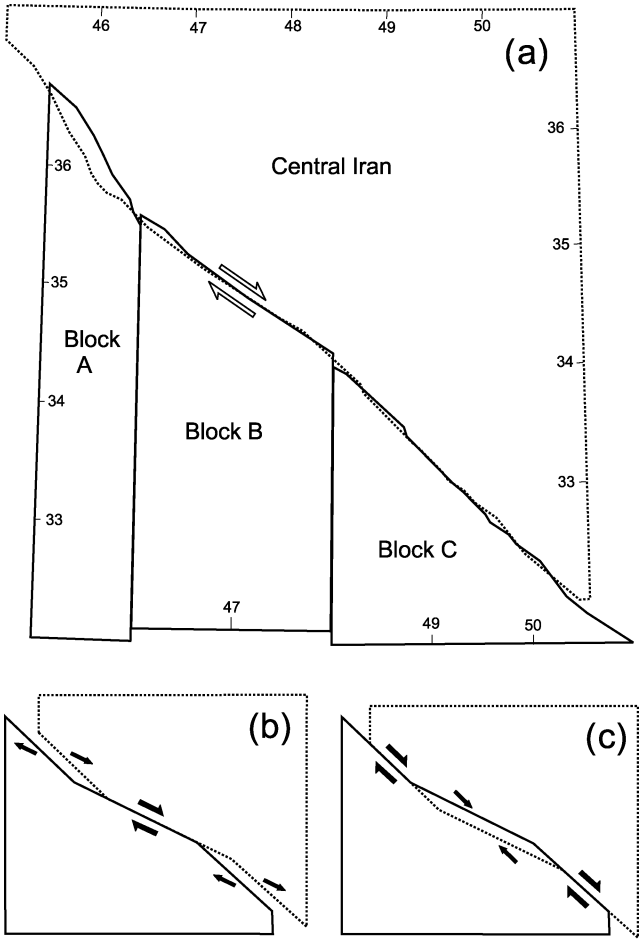

Figure 8. (a) The Main Recent Fault changes its trend between its NW section near Marivan (330°), its middle section near Sahneh (300°) and its SE section near Dorud (315°). Any single slip vector for the whole fault system will lead to components of extension or shortening in some places, as in (b), where the slip vector is parallel to the central section, or in (c), where it is closer to the trend of the NW and SE sections. We have assumed a slip vector that produces an extensional component in the NW section (see text), so that an overlap is created when that section is restored, as in (a), and have allowed the blocks A, B and C south of the fault to be restored separately.

In the Nahavand–Dorud region, Fig. 9(b) shows that the 50 km reconstruction apparently isolates the rivers through Azna and Borujerd (streams G and H) on the NE side of the fault from any possible outlet to the SW. However, it also brings those streams opposite two dry valleys at G (South Nahavand) and H (South Borujerd). The South Nahavand dry valley is shown in Figs 5 and 6 and its pass is now ∼600 m above the Nahavand plain, in a region where the 1958 earthquake faulting and the geomorphology indicate a significant vertical component of slip on the fault, down to the NE. The South Borujerd dry valley forms another pass, this time 500 m above the Dorud plain (Fig. 10). The pass itself is now a broad flat area containing young, almost horizontal, conglomerates at its highest point, probably dating from the time at which it was an active stream (Fig. 10c). Just beyond the pass to the SW is a high village called Khoshk Roud, literally 'dry river'. The Dorud gorge itself (Fig. 4c) is not used in the reconstruction in Fig. 8(b). Today it takes the drainage from both stream systems G and H (Dorud means 'two rivers') after the two air gaps at South Nahavand and South Borujerd (G and H in Fig. 9b) were abandoned. Another abandoned gorge forms a dry valley at I (Fig. 9), suggesting that it was used before the modern Dorud gorge became the dominant exit. At the time of the reconstruction in Fig. 9(b), we imagine that the broad, flat Borujerd–Dorud valley did not exist. It is formed by an extensional component on the Main Recent Fault arising from either a pull-apart location at a right-step in the faulting or from a slightly oblique slip vector. The length of the valley (50–55 km) is very close to the restored offset on the fault in Fig. 9(b) (55 km).

In the central section near Sahneh, the restoration of the Sonqore stream to Kamyaran (A in Fig. 9), which was the original basis for the reconstruction in Fig. 7, also aligns all the other major streams B–E with appropriate outlets on the SW side. In particular, the river north of Nahavand (E) becomes aligned with a deep gorge at Sahneh (Fig. 11) which, although not completely dry today, was clearly made by a catchment much larger than the small stream that now flows though it.

At the NW end of Fig. 7(b), the ∼50 km restoration brings the Sanandaj river, which today flows through a gorge NE of Paveh (Fig. 12a), into alignment with a gorge NW of Paveh (Fig. 12b). It also brings a beheaded stream at B in Fig. 12(a) into alignment with a dry valley at A (Fig. 13). The drainage in the Marivan region can be plausibly aligned with outlets on the SW side (Fig. 12), but in this region the fault system consists of several anastomosing strands that cross the Marivan–Baneh depression and is hard to reconstruct in detail. As at Dorud, we expect that this depression arises from an extensional component on the fault system, and that it did not exist as a topographic low at the time of the reconstruction.

Finally, at the SE end of Fig. 7 the reconstruction explains an apparent anomaly in the present-day drainage pattern. For most of Fig. 7 the divide separating the drainage of central Iran from that of the Zagros–Persian Gulf is about 50 km NE of the Main Recent Fault. However, at 32.5°N it makes a salient, with the headwaters of the Zayandeh Rud, which flows NE to Isfahan, projecting SW and crossing the Main Recent Fault (Fig. 7b). In this region the Main Recent Fault system may consist of more than one strand, but if we restore all the motion on the main strand, the Zayandeh Rud is brought into alignment with a prominent dry valley at Sepestan (K in Figs 14a–c). It seems probable that the Zayandeh Rud once flowed SW across the Zagros (Fig. 14d), but reversed its drainage when uplift on the SW side of the Main Recent Fault caused the Sepestan gorge to be abandoned. This reconstruction would remove the anomaly in the drainage divide (Figs 7b and 14b).

Thus our restoration of ∼50 km, which arose from moving the Sonqore river from the gorge at Dinevar to the next gorge at Kamyaran, also restores the other major stream systems to exits that are either current gorges or abandoned dry valleys. In addition, it accounts for the length of the Dorud–Borujerd pull-apart basin, for the low topography in the Marivan–Baneh area, and for the apparent reversal of drainage in the Zayandeh Rud. Its most obvious weakness is that it leaves the gorge at Dorud itself unoccupied (Fig. 7b), in spite of this being a major exit for the drainage today (Fig. 4c). This can be rectified with a small additional offset, making a total of ∼70 km (Fig. 15). This new offset causes the Dorud gorge to be used and most of the other streams to the NE have appropriate outlets to the SW as well. Some uncertainty exists around the Dorud–Azna region itself because it is not possible to predict in detail where streams crossed what is now the Borujerd–Dorud depression. The only substantial stream with no apparent outlet at the 70 km offset is that through Sonqore.

In summary, the drainage reconstructions provide evidence for a right-lateral offset of approximately 50 km, and possibly as much

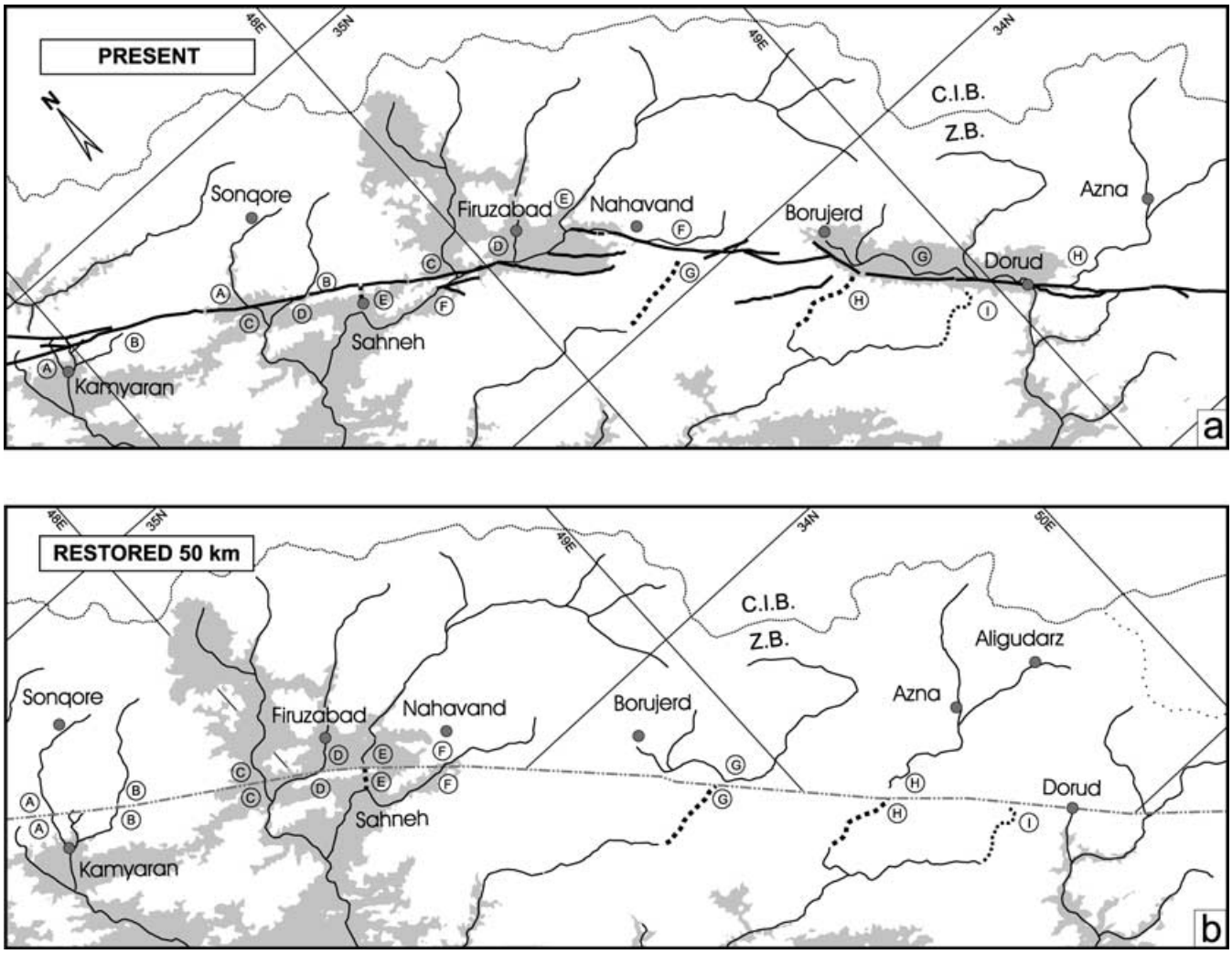

Figure 9. Detail of the present-day (a) and ∼50 km reconstruction (b) of the drainage between Kamyaran and Dorud. Streams A–H on the NE side of the fault in (a) have been matched to gorges or dry valleys A–I on the SW side in (b). Dry valleys are marked by thick dashed lines, while the thin dotted line in the NE is the main drainage divide separating the Zagros Basin (ZB) from the Central Iran Basin (CIB). The thick lines in (a) are the major trances of the Main Recent Fault, while the dashed line in (b) is the approximate line of the fault used in the reconstruction. Shaded areas are lower than 1600 m elevation.

as 70 km. The restored stream patterns are shorter, simpler and flow directly across the line of the Main Recent Fault (Figs 7b and 15), with less of the drainage being trapped along the fault, as it is today between Nahavand and Sahneh and between Borujerd and Dorud (Fig. 7a).

4.2 Geological evidence

Potential offset marker beds occur in two places. The central section between Kamyaran and Sahneh contains distinctive ophiolitic rocks of probable Cretaceous age (Stöcklin 1974; Haynes & McQuillan 1974; Stoneley 1976) that are cut by the Main Recent Fault (Fig. 16). An apparent offset between the two sides of 47 km (between the arrows in Fig. 16) is close to that used to reconstruct the drainage in Figs 7(b) and 9(b) (50 km), though this is not a unique reconstruction of the geology.

In the Dorud region a distinctive structural and stratigraphic package consisting of folded Upper Cretaceous radiolarites bounded by a thrust fault is truncated by the Main Recent Fault south of Borujerd and can be identified again on the other side of the fault SE of Dorud (Fig. 17; Gidon *et al.* 1974). Once again, because the structures are at a low angle to the Main Recent Fault, it is difficult to make a definitive reconstruction. Gidon *et al.* (1974) estimated an offset of ∼60 km in this region, similar to that used to reconstruct the drainage in Figs 7(b) and 9(b) (55 km), and also approximately the same as the length of the Borujerd–Dorud pull-apart basin (50–55 km). The offset between the arrows in Fig. 17, on the apparent 'piercing point' where the northern limb of the anticline is truncated by the fault, is ∼75 km, which is rather larger than the estimate of Gidon *et al.* (1974), but similar to that of the ∼70 km reconstruction in Fig. 15(b) (74 km).

We emphasize that none of the geological estimates of the offsets are precise or unambiguous, as the fault intersects the geological structure at a small angle. Nonetheless, we conclude that the preserved offsets in the geology are not grossly in conflict with our proposed offsets of ∼50 km (and possibly ∼70 km) based on the drainage reconstructions.

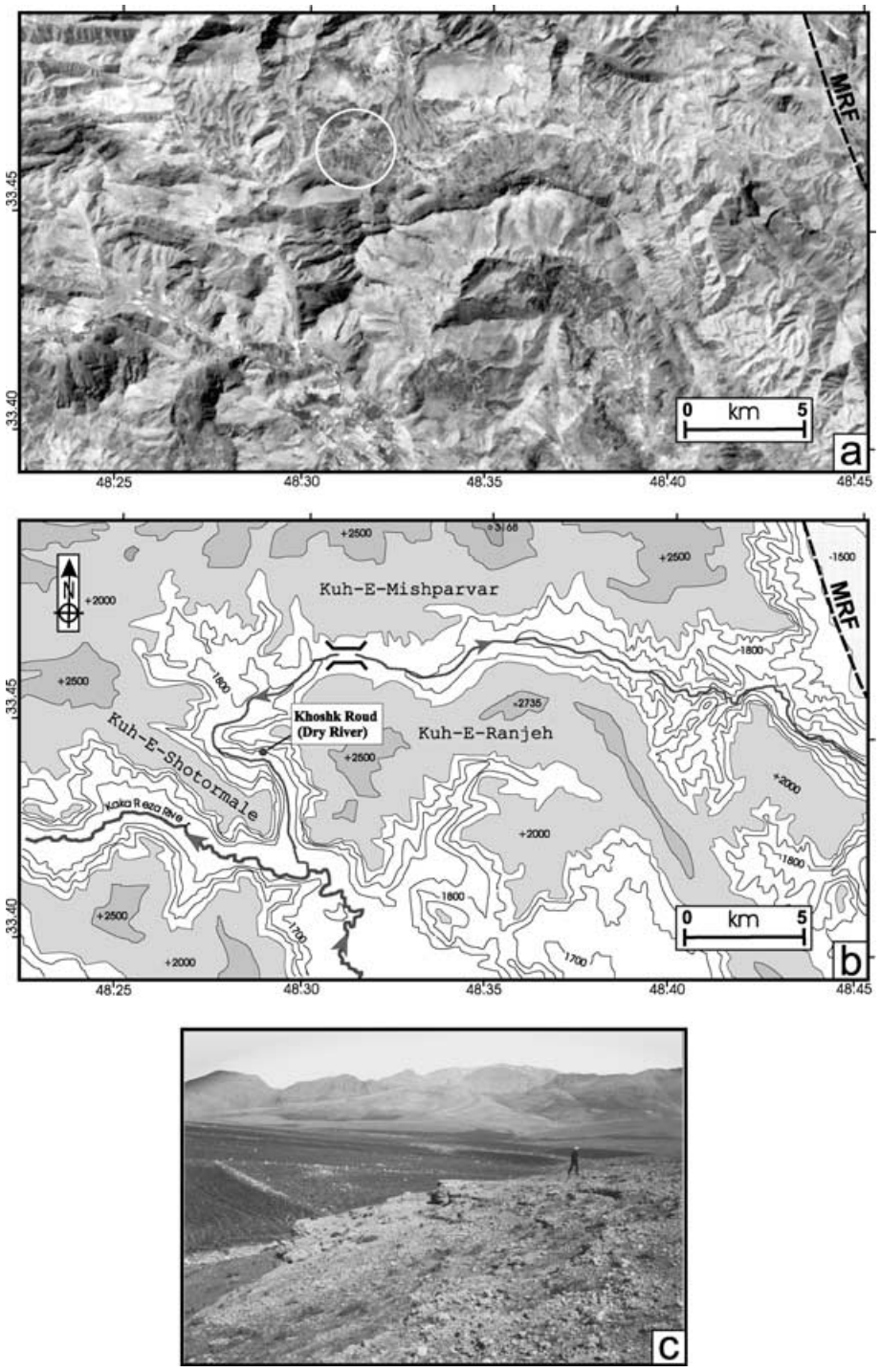

Figure 10. The dry valley south of Borujerd, marked H in Fig. 9. (a) LANDSAT image with the pass itself circled. The trace of the Main Recent Fault is the dashed line in the east. (b) Detailed topographic map of the region in (a). The stream now draining east from the pass is the Sardeh River, whose terraces are cut by the Main Recent Fault where it enters the Dorud basin (Figs 3c and d). (c) View looking north in the pass itself (circled region in Fig. 10a) at 33°46.3′N 48°31.8′E. The person is standing on cemented conglomerates on the now dry watershed.

5 DISCUSSION

Our reconstructions of the drainage patterns and the geology are consistent with a right-lateral strike-slip offset of ∼50 km on the Main Recent Fault. The offset could be extended to ∼70 km without severely affecting the quality of the reconstruction, but the evidence for the extra 20 km is not compelling. The ∼50 km reconstruction restores the drainage pattern to a simple network of short streams that flow straight across the line of the Main Recent Fault, accounts for the length of the Borujerd–Dorud pull-apart basin, and provides an adequate restoration of the few distinctive offset geological units. As offset on the fault increased, the streams crossing it switched or abandoned outlets to give the more complicated drainage pattern seen today, in which some stream systems flow subparallel to the

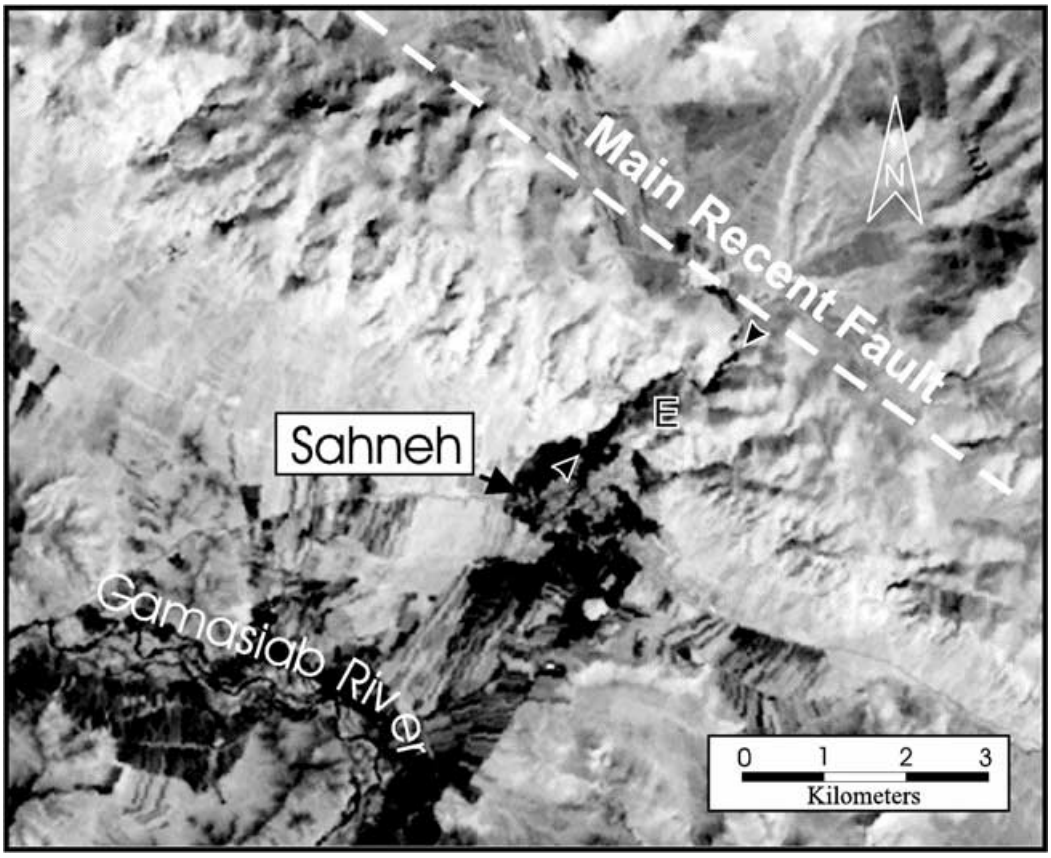

Figure 11. LANDSAT image of the gorge at Sahneh (black arrows), marked E in Fig. 9 and which was deeply incised by a substantial stream flowing SW, but which is now cut-off from any substantial catchment.

fault for tens of kilometres before finding an exit to the SW. Thus the drainage pattern seems to be a result of the fault itself, and not of the rather complicated capture mechanisms that arise further SW in the Simply Folded Belt of the Zagros, which are dominated by effects related to the alternating hard and soft units in the stratigraphy (Oberlander 1965; Oberlander 1968).

The transverse dry valleys that occur on the SW side of the fault are particularly interesting because their presence is necessary to confirm our reconstructions. They occur in sections of the fault that strike 315°–330° (Fig. 18) and are nearly all 500–600 m above their currently adjacent, or previously adjacent, valley floors or rivers. The ∼50 km strike-slip offset is associated with ∼500 m relative vertical motion, showing that the ratio of horizontal to vertical slip on the Main Recent Fault in those sections is about 100.

None of these offsets can, yet, be dated directly. The only constraints on timing are those based on regional geological arguments summarized in Section 2.2. We suspect that the present configuration of faulting in Iran dates from about 3–5 Ma, when there was a substantial reorganization of the tectonics in the South Caspian Basin and the Simply Folded Belt of the Zagros. If the Main Recent Fault also dates from that time then its long-term horizontal slip rate is about 10–17 mm yr^{-1}, with a vertical component of ∼0.1–0.2 mm yr^{-1} in the Dorud region. In this part of the Zagros, where the overall N–S motion is partitioned into NW–SE strike-slip and NE–SW shortening, these rates would imply 14–23 mm yr^{-1} N–S shortening across the NW Zagros, leaving the rest (6–15 mm yr^{-1}) of the Arabia–Eurasia shortening to be taken up elsewhere in NW Iran. At these rates, the Main Recent Fault should be a source of relatively frequent earthquakes of M_s 6–7, as is seen in the historical record (Ambraseys & Melville 1982; Berberian & Yeats 2001).

Some support for these dates, and hence rates, comes from a different argument. Further west in Turkey, the modern slip rate on the North Anatolian Fault is now well-constrained by GPS measurements to be about 24 ± 3 mm yr^{-1} (McClusky *et al.* 2000). The offset on the North Anatolian Fault is also known to be about 80–85 km at both its eastern and western ends (Westaway 1994; Armijo *et al.* 1999). At its western end its age can be constrained by a Pliocene marine transgression that follows the Mediterranean Messinian crisis, dating the onset of faulting to ∼5 Ma or younger (Armijo *et al.* 1999). This gives a long-term slip rate of ∼16 mm yr^{-1} if it started at 5 Ma or 28 mm yr^{-1} if it started at 3 Ma, which brackets the GPS estimates. At the eastern end, it is sometimes claimed that the North Anatolian fault is older, and started about 10 Myr (Şengör *et al.* 1985; Barka 1992). However, this conclusion is based on an assumed connection between Neogene basins and the faulting and on the age of continental sediments that are difficult to date precisely (see e.g. Bellier *et al.* 1997). If the North Anatolian Fault is really younger in the west than in the east (e.g. Armijo *et al.* 1999), it raises the difficult question of how the offset can be the same all along it. Clearly, one possibility is that it is essentially the same age all along its length, and that it has been moving for the last 3–5 Myr at an average rate similar to that seen in the GPS measurements.

If these arguments are correct, the horizontal offset on the Main Recent Fault is not only similar in size (50–70 km versus ∼85 km) but also similar in age to that on the North Anatolian Fault. In this light, it looks increasingly as though the two faults have marked

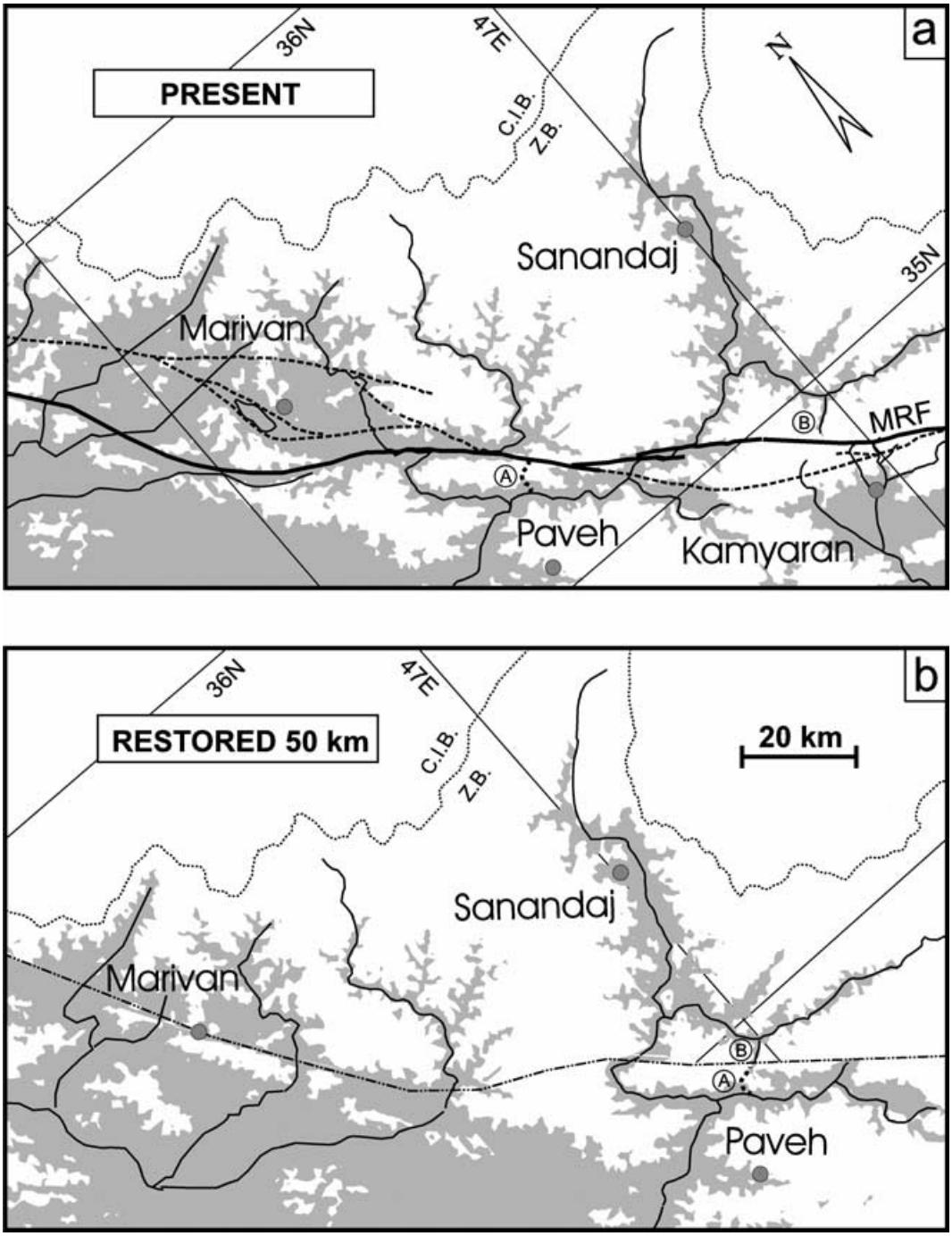

Figure 12. Detail of the present-day (a) and restored (b) drainage pattern in the NW section of the Main Recent Fault, near Marivan. The major trace of the Main Recent Fault system is marked by a thick line in (a), with other faults, which may be inactive, dashed. The approximate course of the fault used in the reconstruction is marked by a dashed line in (b). The reconstruction restores the stream B in (a), which now flows NE, to the dry valley marked A near Paveh. The reconstruction near Marivan itself is conjectural, as this is the area where the low elevation NE of the Main Recent Fault, and the different strike of the fault zone itself, suggest an extensional component of motion, causing the Marivan basin to be destroyed by overlap when the fault offset is restored.

an almost continuous zone of right-lateral shear extending from Istanbul to Isfahan that has been active for the last 3–5 Myr. Its continuity in space is broken only in eastern Turkey and NW Iran, where the shortening component of the Arabia–Eurasia convergence happens to be on the north side of the system, in the Caucasus, rather than on the south (Fig. 1). The offset on the Main Recent Fault can also throw light on the geographical distribution of the Arabia–Eurasia shortening in western Iran. The pattern of active faulting and earthquake slip vectors today leaves little doubt that the N–S Arabia–Eurasia convergence is partitioned into its strike-slip and thrusting components in the NW Zagros. A strike-slip offset of ∼50 km therefore implies an accompanying shortening component that is also ∼50 km. This estimate is compatible with geological estimates of shortening in the Simply Folded Belt of the Zagros since

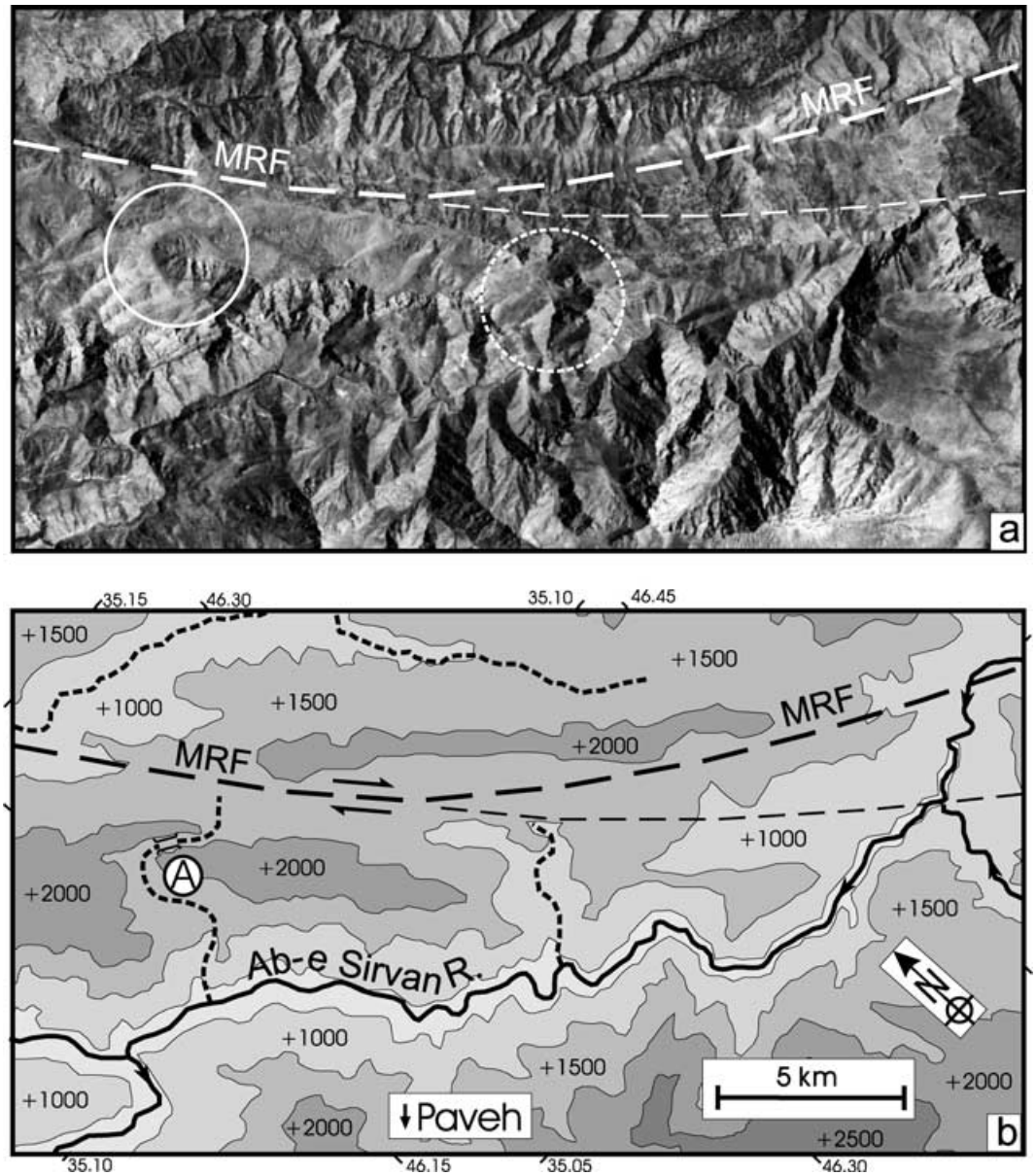

Figure 13. (a) LANDSAT image and (b) map of the stream systems near Paveh, shown in Fig. 12. The main dry valley A in Fig. 12 is the left-hand circle in (a) with another gorge that appears to have lost most of its catchment also ringed on the right. The major trace of the Main Recent Fault is marked by thick dashes.

the early Pliocene (Falcon 1969, 1974). It also implies an overall N–S convergence of ∼70 km. Reassessments of current motions in the Red Sea and Gulf of Aden (Jestin *et al.* 1994; Chu & Gordon 1998) allow better definition of the Arabia–Africa motion than older global models of plate motion (De Mets *et al.* 1994). Such older models consequently also poorly define the Arabia–Eurasia motion. By combining the Africa–Arabia motion of Chu & Gordon (1998) with the Africa–Eurasia motion of De Mets *et al.* (1994), we obtained a pole for the Arabia–Eurasia motion at 30.48°N 13.04°E with an angular rotation rate of 0.518° Myr^{-1}. With this motion, the total Arabia–Eurasia convergence over the last 3–5 Myr is expected to be 85–140 km in a roughly N–S direction at longitude 48°E. We therefore estimate that over this time, the NW Zagros region has accommodated a substantial fraction of that total convergence, leaving only 15–70 km to be taken up further NE in the western Alborz and southern Caspian. The tectonics of those regions is discussed elsewhere (Jackson *et al.* 2002).

6 CONCLUSIONS

We have demonstrated that a right-lateral strike-slip offset of ∼50 km on the Main Recent Fault is compatible with a restoration of the drainage, geological markers and the length of the Borujerd–Dorud pull-apart basin. There is some evidence that the offset may be as much as ∼70 km. The configuration of the active faulting and earthquake slip vectors today shows that this offset is geometrically linked to a shortening of ∼50 km across the NW Zagros and to a total N–S convergence of ∼70 km, which is a substantial fraction of the 85–140 km total Arabia–Eurasia convergence over the last

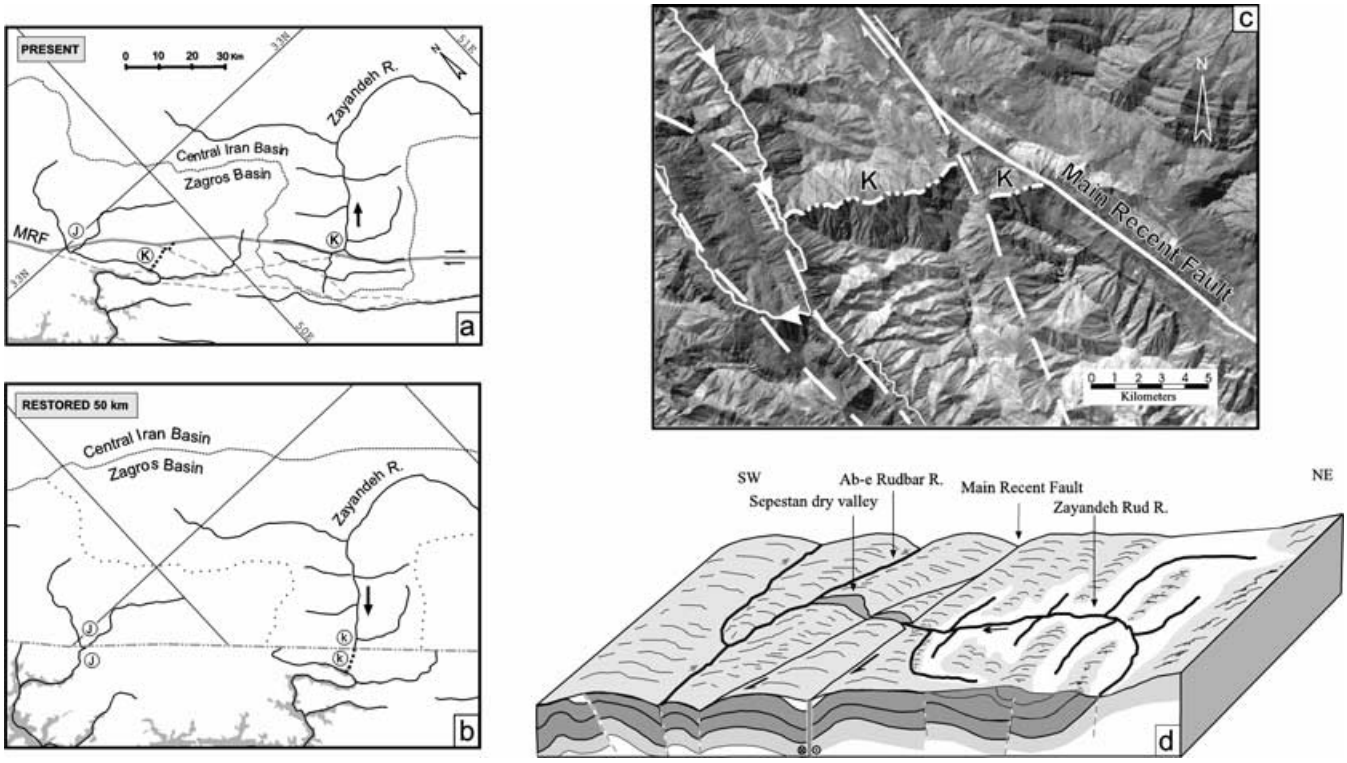

Figure 14. (a) The present-day configuration and (b) the restored drainage system near the head waters of the Zayandeh Rud river, SE of Dorud. The LANDSAT image of the dry valleys marked K on the SW side of the fault in (a) is shown in (c). The Main Recent Fault is marked by the continuous thick line. Other faults, most of which are thrusts of the High Zagros, are dashed. (d) Cartoon of the restored drainage system, showing how the Zayandeh Rud was probably once a stream draining SW to the Persian Gulf, but has reversed its flow as it failed to maintain its course through the SW side of the Main Recent Fault. This would account for the apparent anomaly in the otherwise linear drainage divide between the Zagros basin and central Iran.

3–5 Myr. If the initiation of the Main Recent Fault dates from that time, as seems likely from geological arguments, then its offset and age are similar to those on the North Anatolian Fault in Turkey. The two faults then represent an almost continuous zone of right-lateral shear on the northern margin of the Arabia and Turkish plates that has been active since the Pliocene. The horizontal slip rate on the Main Recent Fault would then be in the range 10–17 mm yr^{-1}, with a vertical component of ~0.1–0.2 mm yr^{-1} in the Dorud region.

In the future we may have better estimates of the age of the Main Recent Fault and its current slip rate will be better determined through GPS measurements. However, measurement of its offset has already demonstrated that the Main Recent Fault is a major structural element in the late Neogene Arabia–Eurasia collision, and that better knowledge of its history and characteristics has important implications for understanding seismic hazard and the active tectonics of Iran.

ACKNOWLEDGMENTS

We thank M. Korehie and M. Ghorashi of the Geological Survey of Iran for their constant support of our research in Iran over many years. MT thanks Amerada Hess, King's College, the Cambridge Overseas Trust and the Foreign & Commonwealth Office for

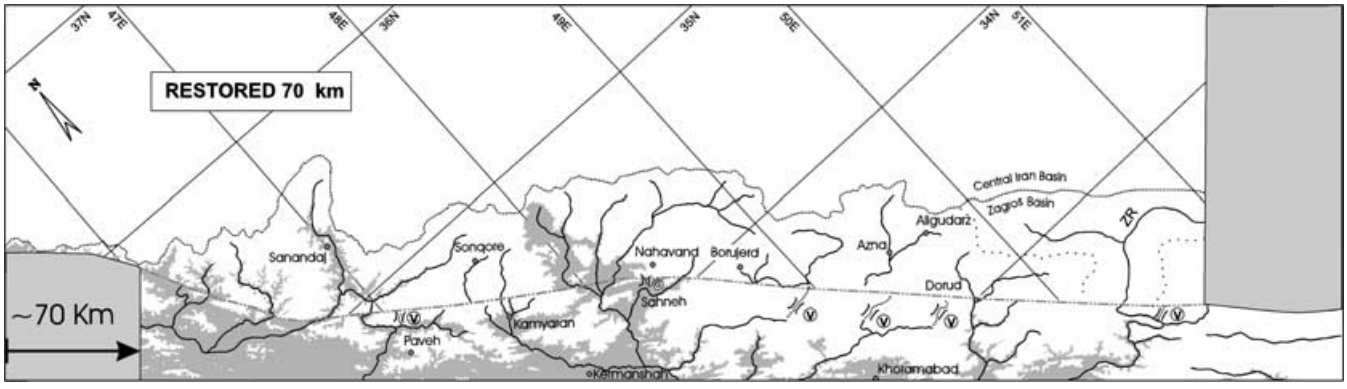

Figure 15. Restored drainage configurations with an offset of ~70 km on the Main Recent Fault (see text). Notation and shading are as in Fig. 7.

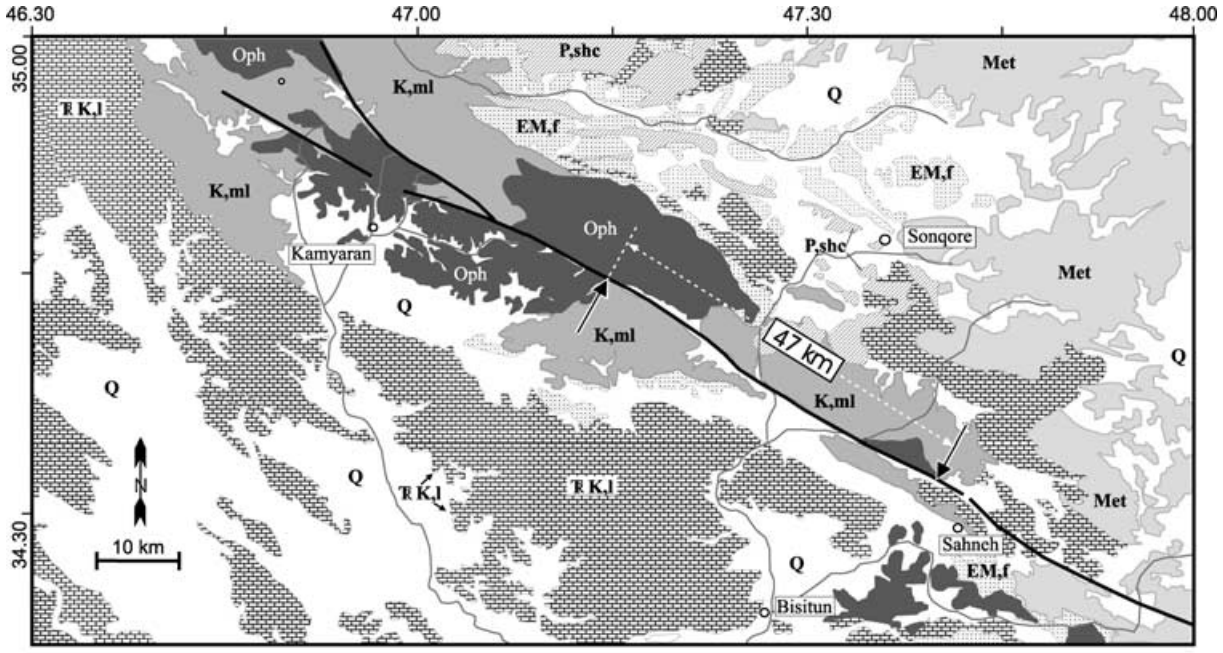

Q: Quaternary deposits
EM,f: Eocene to Miocene flysh
P,shc: Paleocene shale, sandstone and conglomerate
Oph: Ophiolitic rocks
K,ml: Cretaceous marl, limestone and shale (slate)
ℜ K,l: Triassic to Cretaceous thick bedded to massive Orbitolina limestone
Met: Undifferentiated metamorphic rocks

Figure 16. Summary geological map of the Kamyaran–Sahneh region, showing the possible offset of distinctive ophiolitic rocks. Simplified from various 1:250 000 and 1:100 000 maps of the Geological Survey of Iran.

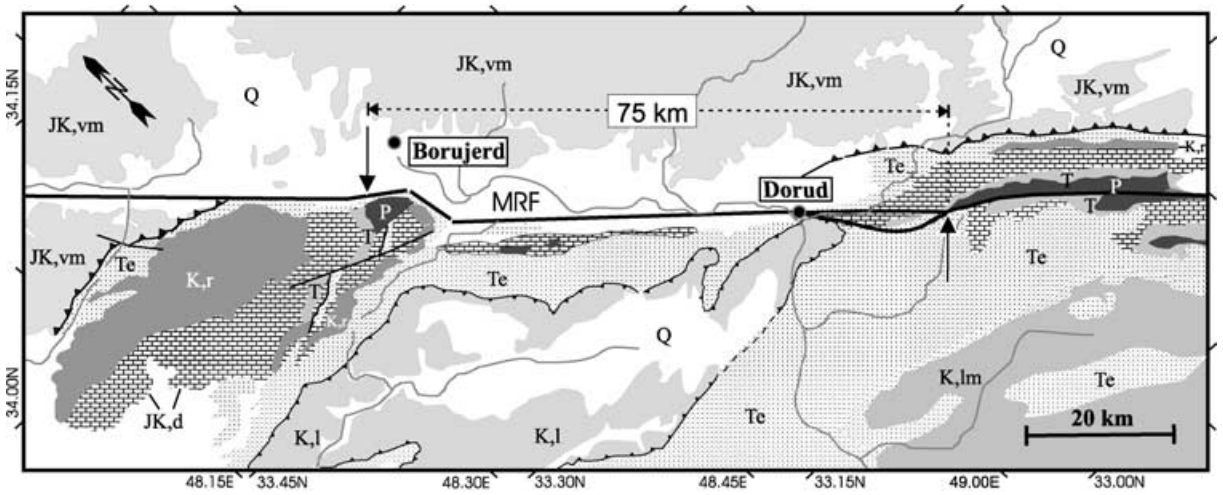

Q: Quaternary deposits
Te: Tertiary shale, sand stone, conglomerate and limestone
K,lm: Cretaceous thin-bedded limestone and blue marly limestone
K,l: Cretaceous rudist and Orbitolina limestone
K,r: Cretaceous radiolarite, limestone and shale
JK,vm: Jurassic to Cretaceous Orbitolina limestone, volcanic and metamorphic rocks
JK,d: Thick to medium bedded dolomite and limestone
T: Triassic marl and limestone
P: Paleozoic dolomite

Figure 17. Summary geological map of the Borujerd–Dorud area, showing the possible offset of distinctive geological units (see also Gidon *et al.* 1974). Simplified from various 1:250 000 and 1:100 000 maps of the Geological Survey of Iran.

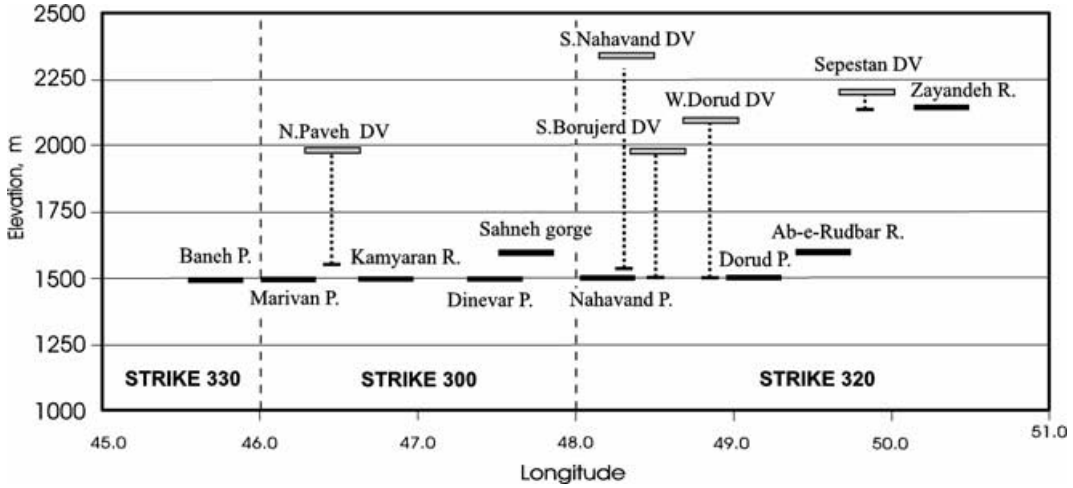

Figure 18. Summary of the elevations of gorges and dry valleys along the Main Recent Fault. Entrances to gorges are shown as black lines. Dry valleys are grey lines, linked by dotted lines to the elevations of their adjacent valleys on the NE side of the fault in the restored drainage configuration (Fig. 7b). Note how most of the dry valleys occur in the SE, associated with the Borujerd–Dorud basin or in the NW near the Marivan depression. In both places the vertical component on the Main Recent Fault system is enhanced, probably by an extensional or normal component. Most of the dry valleys are about 500 m above their originally adjacent basins, but the Zayandeh Rud is close to the elevation of the Sepestan dry valley, suggesting little vertical component in that part of the fault zone.

scholarships enabling him to study in Cambridge. We are grateful to M. Allen, O. Bellier, M. Berberian, D. McKenzie and S. McClusky for helpful reviews, though we alone are responsible for any remaining errors. This work was supported by the NERC Centre for Modelling and Observation of Earthquakes and Tectonics (COMET) Cambridge Earth Sciences contribution ES 6753.

REFERENCES

Ambraseys, N.N. & Melville, C.P., 1982. *A History of Persian Earthquakes,* Cambridge Univ. Press, New York, p. 219.

Ambraseys, N. & Moinfar, A., 1973. The seismicity of Iran: the Silakhor (Lurestan) earthquake of 23rd January 1909, *Ann. Geophys.,* **26**, 659–678.

Ambraseys, N. & Moinfar, A., 1974a. The seismicity of Iran: the Firuzabad (Nehavand) earthquake of 16th August 1958, *Ann. Geophys.,* **27**, 1–21.

Ambraseys, N. & Moinfar, A., 1974b. The seismicity of Iran: the Karkhaneh (Kangavar) earthquake of 24th March 1963, *Ann. Geophys.,* **27**, 23–36.

Ambraseys, N., Moinfar, A. & Peronaci, F., 1973. The seismicity of Iran: the Farsinaj (Kermanshah) earthquake of 13th December 1957, *Ann. Geophys.,* **26**, 679–692.

Armijo, R., Meyer, B., Hubert, A. & Barka, A., 1999. Westward propagation of the North Anatolian fault into the northern Aegean: timing and kinematics, *Geology,* **27**, 267–270.

Barka, A.A., 1992. The North Anatolian fault zone, *Ann. Tectonicae,* special issue **6**, 164–195.

Bellier, O., Över, Poisson, A. & Andrieux, J., 1997. Recent temporal change in the stress state and modern stress field along the North Anatolian Fault Zone (Turkey), *Geophys. J. Int.,* **131**, 61–86.

Berberian, M., 1995. Master blind thrust faults hidden under the Zagros folds: active basement tectonics and surface morphotectonics, *Tectonophysics,* **241**, 193–224.

Berberian, M. & King, G., 1981. Towards a paleogeography and tectonic evolution of Iran, *Can. J. Earth Sci.,* **18**, 210–265.

Berberian, M. & Yeats, R.S., 2001. Contribution of archaeological data to studies of earthquake history in the Iranian Plateau, *J. Struct. Geol.,* **23**, 563–584.

Chu, D. & Gordon, R.G., 1998. Current plate motions across the Red Sea, *Geophys. J. Int.,* **135**, 313–328.

DeMets, C., Gordon, R.G., Argus, D.F. & Stein, S., 1994. Effects of recent revision to the geomagnetic reversal timescale on estimates of current plate motions, *Geophys. Res. Lett.,* **21**, 2191–2194.

Devlin, W.J., Cogswell, J.M., Gaskins, G.M., Isaksen, G.H., Pitcher, D.M., Puls, D.P., Stanley, K.O. & Wall, G.R.T., 1999. South Caspian basin: young, cool, and full of promise, *GSA Today,* **9**, 1–9.

Dewey, J.F., Hempton, M.R., Kidd, W.S.F., Şaroğlu, F. & Şengör, A.M.C., 1986. Shortening of continental lithosphere: the neotectonics of Eastern Anatolia, a young collision zone, in *Collision Tectonics,* eds Coward, M.P. & Ries A.C., *Geol. Soc. Spec. Publ. London,* **19**, 3–36.

Engdahal, E.R., van der Hilst, R. & Buland, R., 1998. Global teleseismic earthquake relocation with improved traveltimes and procedures for depth determination, *Bull. seism. Soc. Am.,* **88**, 722–743.

Falcon, N.L., 1969. Problems of the relationship between surface structure and deep displacements illustrated by the Zagros Range, in *Time and Place in Orogeny, Geol. Soc. Spec. Publ. London,* **3**, 9–22.

Falcon, N.L., 1974. Southern Iran: Zagros Mountains, in *Mesozoic–Cenozoic Orogenic Belts, Data for Orogenic Studies,* ed. Spencer, A.M., *Geol. Soc. Spec. Publ. London,* **4**, 199–211.

Gidon, M., Berthier, F., Billiault, J.P., Halbronn, B. & Maurizot, P., 1974. Sur le carateres et l'ampleur du coulissement de la 'Main Fault' dans la region de Borujerd-Dorud, Zagros oriental, Iran, *C.R. Acad. Sci., Paris, Ser. D.,* **278**, 701–704.

Haynes, S.J. & McQuillan, H., 1974. Evolution of the Zagros suture zone, southern Iran, *Bull. geol. Soc. Am.,* **85**, 739–744.

Hempton, M.R., 1987. Constraints on Arabian plate motion and extensional history of the Red sea, *Tectonics,* **6**, 687–705.

Jackson, J., 1992. Partitioning of strike-slip and covergent motion between Eurasia and Arabia in eastern Turkey and the Caucasus, *J. geophys. Res.,* **97**, 12 471–12 479.

Jackson, J., 1999. Fault death: a prespective from actively deforming regions, *J. Struct. Geol.,* **21**, 1003–1010.

Jackson, J., 2001. Living with earthquakes: know your faults, *J. Erthq. Eng.,* **5**, special issue 1, 5–123.

Jackson, J.A. & Ambraseys, N.N., 1997. Convergence between Eurasia and Arabia in eastern Turkey and the Caucasus, in *Historical and Prehistorical Earthquakes in the Caucasus,* pp. 79–90, eds Giardini, D. & Balassanian, S., Kluwer, Dordrecht.

Jackson, J. & McKenzie, D., 1984. Active tectonics of the Alpine–Himalayan belt between western Turkey and Pakistan, *Geophys. J. R. astr. Soc.,* **77**, 185–264.

Jackson, J., Priestley, K., Allen, M.B. & Berberian, M., 2002. Active tectonics of the South Caspian Basin, *Geophys. J. Int.,* **148**, 214–245.

Jestin, F., Huchon, P. & Gaulier, J.M., 1994. The Somalia plate and the East African rift system: present-day kinematics, *Geophys. J. Int.,* **116**, 637–654.

McCall, G.J.H., 1996. The inner Mesozoic to Eocene ocean of south and central Iran and associated microcontinents, *Geotectonics,* **29**, 490–499.

McClusky, S. *et al.*, 2000. GPS constrains on plate motions and deformations in the Eastern Mediteranean: implication for plate dynamics, *J. geophys. Res.,* **105**, 5695–5719.

McKenzie, D.P., 1972. Active tectonics of the Mediterranean region, *Geophys. J. R. astr. Soc.,* **30**, 109–185.

McKenzie, D.P. & Jackson, J.A., 1983. The relation between strain rates, crustal thickening, paleomagnetism, finite strain and fault movements within a deforming zone, *Earth planet. Sci. Lett.,* **65**, 182–202.

Molnar, P. & Gipson, J.M., 1994. Very long baseline interferometry and active rotations of crustal blocks in the Western Transverse Ranges, California, *Bull. geol. Soc. Am.,* **106**, 594–606.

Oberlander, T.M., 1965. The Zagros streams, *Syracuse Geogr. Ser. 1,* Syracuse Univ. Press, p. 168.

Oberlander, T.M., 1968. The origin of the Zagros defiles, in *The Cambridge History of Iran,* pp. 195–211, ed. Fisher, W.B., Cambridge Univ. Press, Cambridge.

Replumaz, A., Lacassin, R., Tapponnier, P. & Leloup, P.H., 2001. Large river offsets and Plio-Quaternary dextral slip rate on the Red River fault (Yunnan, China), *J. geophys. Res.,* **106**, 819–836.

Şengör, A.M.C., Görür, N. & Şaroğlu, F., 1985. Strike-slip faulting and related basin formation in zones of tectonic escape: Turkey as a case study, in *Strike-Slip Faulting and Basin Formation, Spec. Publ., 37,* eds Biddle, K. & Christie-Blick, N., Society of Economic Paleontologists and Mineralogists, Tulsa, Okla.

Shirakova, E.I., 1967. General features in the orientation of principal stresses in earthquake foci in the Mediterranean–Asian seismic belt, *Earth Phys.,* **1**, 22–36.

Stöcklin, J., 1974. Possible ancient continental margins in Iran, in *The Geology of Continental Margins,* pp. 873–887, eds Burke, C.A. & Drake, C.L., Springer-Verlag, New York.

Stoneley, R., 1976. On the origin of ophiolite complexes in the southern Tethys region, *Tectonophysics,* **25**, 303–322.

Stoneley, R., 1981. The geology of the Kuh-e-Dalneshin area of southern Iran, and its bearing on the evolution of southern Tethys, *J. geol. Soc. Lond.,* **138**, 509–526.

Tchalenko, J.S. & Braud, J., 1974. Seismicity and structure of the Zagros: the Main Recent Fault between 33° and 35°N, *Phil. Trans. R. Soc. Lond.,* A., **277**, 1–25.

Walker, R. & Jackson, J., 2002. Offset and evolution of the Gowk fault, S.E. Iran: a major intracontinental strike-slip system, *J. Struct. Geol.,* in press.

Wellman, H.W., 1966. Active wrench faults of Iran, Afghanistan and Pakistan, *Geol. Rundsch.,* **55**, 716–735.

Westaway, R., 1994. Present-day kinematics of the Middle East and eastern Mediterranean, *J. geophys. Res.,* **99**, 12 071–12 090.